Available online at www.sciencedirect.com
SCIENCE DIRECT
Vision Research 46 (2006) 3259–3266
Vision Research
www.elsevier.com/locate/visres

The optics of vertebrate photoreceptors: Anisotropy and form birefringence

N.W. Roberts

School of Physics and Astronomy, University of Manchester, Manchester M13 9PL, UK

Received 12 September 2005; received in revised form 17 March 2006

Abstract

The optics of vertebrate photoreceptors have been investigated with specific reference to the effect of form birefringence. The complex dielectric tensor of the lamellar-like outer segment structure has been derived, allowing the transverse spectral absorbance to be calculated for different incident polarizations. These results were used to calculate the changes in the cellular dichroic ratio as a function of both the volume occupied by the bilayers and the real and complex parts of the intrinsic birefringence of the bilayers. Physiologically realistic values of these parameters show the cellular dichroic ratio to be greater than the bilayer dichroic ratio by a factor of ≈1.3. Furthermore, the calculations of spectral absorbance indicate that form birefringence may affect measurements of optical density in transversely orientated outer segments.

Keywords: Vertebrate photoreceptors; Optical modeling; Form birefringence; Form dichroism; Microspectrophotometry

1. Introduction

For many years it has been known that vertebrate photoreceptors display some intriguing fundamental optical properties that are central to the way they function (Harosi, 1981; Laughlin, Menzel, & Snyder, 1975). The absorption of light by both rods and cones is not only governed by the specific bio-chemical nature of the opsin–chromophore relationship, but also by the physical structure of the cell (Harosi, 1981; Israelachvili, Sammut, & Snyder, 1975). Optical properties such as intrinsic birefringence, dispersion, real and complex form birefringence all arise because of the structure of the self assembled lipid bilayer stack in the outer segment. Understanding the effects of these optical properties has become essential for both the correct interpretation of many different types of experimental measurements and understanding some sensory specializations such as polarization sensitivity.

Microspectrophotometry (MSP) is the major experimental technique for measuring both the spectral absorbance of individual cells and their dichroic ratios; the latter defined as the ratio between the absorbance of light linearly polarized parallel and perpendicular to the plane of the bilayers in the outer segments (Harosi, 1981). Considerable success has been achieved in using measured values of the dichroic ratio to provide information on such quantities as visual pigment concentrations (Harosi, 1975, 1981) and orientation of the chromophore within the bilayer (Harosi & Malerba, 1975; Liebman, 1962; Roberts, Temple, Haimberger, Gleeson, & Hawryshyn, 2004). Even so, Haggins and Jennings (1959) were the first to recognize that dichroic ratio measurements do not provide direct information on the absorbance in the bilayers due to the effects of form birefringence. Form birefringence occurs in a layered system such as the outer segment of a rod or a cone because of the continuous boundary conditions imposed by Maxwell's equations at the bilayer/cytoplasm interfaces. Several works by Moody (1964), Weale (1971), Laughlin et al. (1975), Israelachvili et al. (1975), Snyder and Laughlin (1975) and Harosi (1981) have since

E-mail address: nicholas.roberts@manchester.ac.uk

0042-6989/$ - see front matter © 2006 Elsevier Ltd. All rights reserved.
doi:10.1016/j.visres.2006.03.019

attempted to calculate theoretically the effect of form birefringence on the optics of the cell. However, although all of these works have provided some excellent insight into the problem, no theory has yet provided a complete description of form birefringence within a framework which directly relates to experimental measurements. Furthermore, there are still some inconsistencies between the theories (Harosi, 1978; Snyder, 1978).

A generalized theory of form birefringence was recently deduced by Bêche and Gaviot (2003), the first to use a tensorial approach to describe both uniaxial layered systems (such as the traditional example of a stack of glass plates) and biaxial systems. Roberts and Gleeson (2004) showed that experimentally measured transverse absorbance spectra from vertebrate photoreceptors could be accurately predicted through a combination of defining a complex biaxial dielectric tensor of the outer segment bilayers and accounting for the form birefringence in the system.

In this paper, we set out the complete theory for form birefringence in vertebrate outer segments. In particular, we show that this method allows the direct determination of the spectral dichroic ratios and provides a method for investigating the changes in absorbance that occur as a function of the layered structure. We discuss all these predictions in the context of current experimental measurements.

2. The effective dielectric tensor of the photoreceptor outer segment

Both real and imaginary form birefringence has been well-documented in a variety of periodic dielectric structures (Born & Wolf, 1999, and reference therein). Wiener (1912) first showed that a stack of thin, non-absorbing, isotropic dielectric plates would exhibit effective anisotropic dielectric constants when the thicknesses of the plates and the dimensions of the overall structure were smaller and larger, respectively, than the wavelength of light. Such birefringence is solely due to the nature of the boundary conditions imposed on the electric and displacement field vectors of the light by Maxwell's equations. More complex structures, such as the anisotropic and dichroic bilayer stack in an outer segment, exhibit similar boundary conditions. However, typical derivations of the effective dielectric constants, such as derived in Born and Wolf (1999) and those used by Israelachvili et al. (1975) and Harosi (1981), are only valid for uniaxial systems, where the elements of a dielectric tensor $\epsilon_{ij} = 0$ for $i \neq j$. Bêche and Gaviot (2003) have recently set out a general theory for calculating the effective dielectric tensor of a multi-layer periodic stack for both uniaxial and biaxial dielectric tensors.

Fig. 1A is a schematic diagram of a rod photoreceptor, defining both the tensor quantities and the absorbancies to be used in the following derivations. In the figure, the cellular absorbancies that would be measured experimentally are represented by a_{perp} and a_{par} perpendicular and parallel to the plane of the bilayers. ϵ^{cell} represents the effective

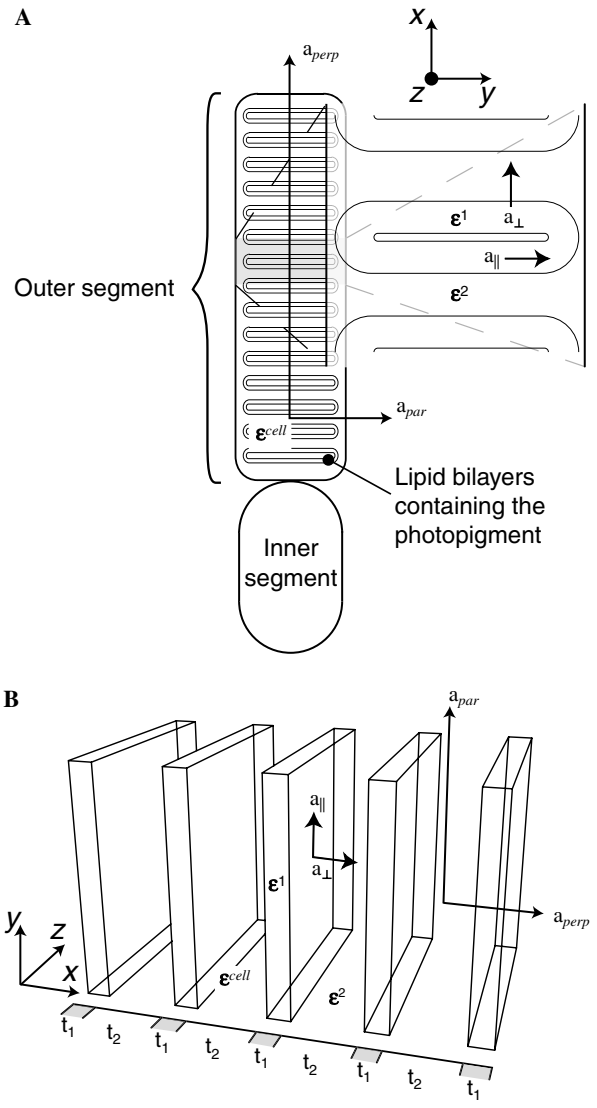

Fig. 1. (A) A schematic diagram of a rod photoreceptor illustrating the lamellar structure of the outer segment. a_{perp} and a_{par} represent the cellular absorbance perpendicular and parallel to the plane of the bilayers. ϵ^{cell} represents the effective dielectric tensor of the outer segment. In the expanded view of the bilayers, $a_{\perp}$ and $a_{\parallel}$ represent the local absorbance of the bilayer perpendicular and parallel to the plane of that bilayer. ϵ^1 and ϵ^2 represent the dielectric tensors of the bilayer and cytoplasm, respectively. (B) Shows a 3D diagram of the structure used to model the outer segment and derive the effective dielectric tensor. Definitions are as in (A) with t_1 and t_2 representing the thicknesses of the bilayers and cytoplasm, respectively.

dielectric tensor of the outer segment. In the expanded view of the bilayers, $a_{\perp}$ and $a_{\parallel}$ represent the local absorbance of the individual bilayers perpendicular and parallel to the plane of that bilayer. ϵ^1 and ϵ^2 represent the dielectric tensors of the bilayer and cytoplasm, respectively. It is assumed here that the local optical properties of the intra- and interdiscal spaces are the same. Fig. 1B further depicts the two length scales of the outer segment, the thicknesses of the bilayer, t_1 and the adjacent cytoplasm t_2. These thicknesses allow the volume fractions of the bilayers, f_1, and the cytoplasm, f_2, to be expressed as

$$f_1 = \frac{t_1}{t_1 + t_2}, \quad f_2 = \frac{t_2}{t_1 + t_2}. \tag{1}$$

For light incident on outer segments in a transverse orientation, for both the bilayers and surrounding cytoplasm the displacement field vectors, **D**, and the electric field vectors, **E**, in the cell are linked to the dielectric tensor, ϵ, by the basic relationship

$$D_l^w = \sum_{k=1}^{M} \epsilon_{lk}^w E_k^w \quad (w = 1 \text{ or } 2), \tag{2}$$

where $k = 1$ to M and $M = 3$ and k stands for the three indices 1, 2, 3, representing an orthogonal x, y, z coordinate system. l stands for each of the x, y, and z directions in turn. Importantly both dielectric tensors show the symmetry $\epsilon_{ij} = \epsilon_{ji}$.

Examining the case where light propagates along the z-axis, defined in both Figs. 1A and B, and adapting the workings of Bêche and Gaviot (2003) for N types of layer, the continuous boundary conditions of the tangential component of the electric field and the normal component of the displacement field across the surface discontinuity result in the general matrix expressions:

$$\mathbf{E}^{\text{cell}} = \sum_{n=1}^{N} \mathbf{G}^n \mathbf{E}^n \text{ with } \mathbf{G}^n = \begin{pmatrix} f_n & 0 & 0 \\ 0 & \frac{1}{N} & 0 \\ 0 & 0 & \frac{1}{N} \end{pmatrix} (n = 1 \text{ to } N) \tag{3}$$

and

$$\mathbf{D}^{\text{cell}} = \sum_{n=1}^{N} \mathbf{P}^n \mathbf{D}^n \text{ with } \mathbf{P}^n = \begin{pmatrix} \frac{1}{N} & 0 & 0 \\ 0 & f_n & 0 \\ 0 & 0 & f_n \end{pmatrix} = \frac{f_n}{N} (\mathbf{G}^n)^{-1} \tag{4}$$

with

$$\mathbf{V}^1\mathbf{E}^1 = \cdots = \mathbf{V}^n\mathbf{E}^n = \cdots = \mathbf{V}^N\mathbf{E}^N$$

$$\text{with } \mathbf{V}^n = \begin{pmatrix} \epsilon_{11}^n & \epsilon_{21}^n & \epsilon_{31}^n \\ 0 & 1 & 0 \\ 0 & 0 & 1 \end{pmatrix} (n = 1 \text{ to } N). \tag{5}$$

From these relations the general matrix expression for the effective dielectric tensor of the periodic system, ϵ^{eff}, becomes

$$\epsilon^{\text{eff}} = \left[\sum_{n=1}^{N} \mathbf{P}^n \epsilon^n (\mathbf{V}^n)^{-1} \mathbf{V}^1 \right] \left[\sum_{n=1}^{N} \mathbf{G}^n (\mathbf{V}^n)^{-1} \mathbf{V}^1 \right]^{-1}. \tag{6}$$

This expression divides into a general set of laws providing a simple way to calculate each element, $\epsilon_{ij}^{\text{eff}}$, of the effective dielectric tensor for any layered structure ($n = 2$ to N):

$$\epsilon_{11}^{\text{eff}} = \frac{\prod_{i=1}^{N} \epsilon_{11}^i}{\sum_{i=1}^{N} \left\{ f_i \left(\prod_{j=1 \neq i}^{N} \epsilon_{11}^j \right) \right\}}, \tag{7}$$

$$\epsilon_{uv}^{\text{eff}} = \frac{\sum_{i=1}^{N} \left\{ f_i \epsilon_{uv}^i \left(\prod_{j=1 \neq i}^{N} \epsilon_{11}^j \right) \right\}}{\sum_{i=1}^{N} \left\{ f_i \left(\prod_{j=1 \neq i}^{N} \epsilon_{11}^j \right) \right\}} \quad (uv = 21, 31), \tag{8}$$

and

$$\epsilon_{uv}^{\text{eff}} = \sum_{i=1}^{N} \{ f_i \epsilon_{uv}^i \} - \sum_{i=1}^{N} \left\{ f_i \frac{\epsilon_{u1}^i \epsilon_{v1}^i}{\epsilon_{11}^i} \right\} + \frac{\left[\sum_{i=1}^{N} \left\{ f_i \epsilon_{u1}^i \left(\prod_{j=1 \neq i}^{N} \epsilon_{11}^j \right) \right\} \right] \left[\sum_{i=1}^{N} \left\{ f_i \epsilon_{v1}^i \left(\prod_{j=1 \neq i}^{N} \epsilon_{11}^j \right) \right\} \right]}{\left[\sum_{i=1}^{N} \left\{ f_i \left(\prod_{j=1 \neq i}^{N} \epsilon_{11}^j \right) \right\} \right] \left[\prod_{i=1}^{N} \epsilon_{11}^i \right]} \tag{9}$$

(for $uv = 22, 23, 33$).

Simplifying these expressions to the case of the outer segment structure where $N = 2$, the effective dielectric tensor of the cell, ϵ^{cell} becomes

$$\begin{aligned}
\epsilon_{11}^{\text{cell}} &= \frac{\epsilon_{11}^1 \epsilon_{11}^2}{f_1 \epsilon_{11}^2 + f_2 \epsilon_{11}^1}, \\
\epsilon_{21}^{\text{cell}} &= \frac{f_1 \epsilon_{21}^1 \epsilon_{11}^2}{f_1 \epsilon_{11}^2 + f_2 \epsilon_{11}^1}, \\
\epsilon_{31}^{\text{cell}} &= \frac{f_1 \epsilon_{31}^1 \epsilon_{11}^2}{f_1 \epsilon_{11}^2 + f_2 \epsilon_{11}^1}, \\
\epsilon_{22}^{\text{cell}} &= f_1 \epsilon_{22}^1 + f_2 \epsilon_{22}^2 - \left(f_1 \frac{\epsilon_{21}^1 \epsilon_{21}^1}{\epsilon_{11}^1} \right) + \frac{\left(f_1 \epsilon_{21}^1 \epsilon_{11}^2 \right)^2}{(f_1 \epsilon_{11}^2 + f_2 \epsilon_{11}^1)(\epsilon_{11}^1 \epsilon_{11}^2)}, \\
\epsilon_{32}^{\text{cell}} &= f_1 \epsilon_{32}^1 - \left(f_1 \frac{\epsilon_{31}^1 \epsilon_{21}^1}{\epsilon_{11}^1} \right) + \frac{\left(f_1 \epsilon_{31}^1 \epsilon_{11}^2 \right)\left(f_1 \epsilon_{21}^1 \epsilon_{11}^2 \right)}{(f_1 \epsilon_{11}^2 + f_2 \epsilon_{11}^1)(\epsilon_{11}^1 \epsilon_{11}^2)}, \\
\epsilon_{33}^{\text{cell}} &= f_1 \epsilon_{33}^1 + f_2 \epsilon_{33}^2 - \left(f_1 \frac{\epsilon_{31}^1 \epsilon_{31}^1}{\epsilon_{11}^1} \right) + \frac{\left(f_1 \epsilon_{31}^1 \epsilon_{11}^2 \right)^2}{(f_1 \epsilon_{11}^2 + f_2 \epsilon_{11}^1)(\epsilon_{11}^1 \epsilon_{11}^2)}
\end{aligned} \tag{10}$$

and where the bilayer and cytoplasm dielectric tensors derived by Roberts and Gleeson (2004) are,

$$\epsilon^1 = \begin{pmatrix} AA & BB & DD \\ BB & CC & EE \\ DD & EE & FF \end{pmatrix} \tag{11}$$

$$\epsilon^2 = \begin{pmatrix} \epsilon_{\text{cytoplasm}} & 0 & 0 \\ 0 & \epsilon_{\text{cytoplasm}} & 0 \\ 0 & 0 & \epsilon_{\text{cytoplasm}} \end{pmatrix} \tag{12}$$

with the elements $AA \ldots FF$ defined in Table 1. Clearly if the dielectric tensor of the bilayer was uniaxial, as assumed in previous theories (i.e., $\epsilon_{ij} = 0$ when $i \neq j$), then the above equations would reduce to the classical solutions of $\epsilon_{11}^{\text{cell}} = (\epsilon_{11}^1 \epsilon_{11}^2)/(f_1 \epsilon_{11}^2 + f_2 \epsilon_{11}^1)$ and $\epsilon_{22}^{\text{cell}} = f_1 \epsilon_{22}^1 + f_2 \epsilon_{22}^2$. It is also perhaps worth noting at this point that by extending the theory to account for the dielectric tensors of the system, the discussions of Harosi (1978) and Snyder (1978) are no longer applicable.

Following then methods set out by Roberts and Gleeson (2004), the derivation of the effective dielectric tensor in turn allows Maxwell's equations to be solved using a

Table 1
Derived elements of the bilayer dielectric tensor from Roberts and Gleeson (2004)

	Elements of the dielectric tensor	
$AA = A$	$A = a\cos^2\gamma - 2b\cos\gamma\sin\gamma + c\sin^2\gamma$	$a = \epsilon_1 + \alpha\sin^2\theta$
$BB = B\cos\tau - D\sin\tau$	$B = b\cos^2\gamma - b\sin^2\gamma + (a-c)\sin\gamma\cos\gamma$	$b = -\alpha\sin\theta\cos\theta\cos\xi$
$CC = C\cos^2\tau - 2E\cos\tau\sin\tau + F\sin^2\tau$	$C = a\sin^2\gamma - 2b\cos\gamma\sin\gamma + c\cos^2\gamma$	$c = (\epsilon_2 + \alpha\cos^2\theta)\cos^2\xi + \epsilon_3\sin^2\xi$
$DD = B\sin\tau + D\cos\tau$	$D = d\cos\gamma - e\sin\gamma$	$d = -\alpha\sin\theta\cos\theta\sin\xi$
$EE = E\cos^2\tau - E\sin^2\tau + (C-F)\sin\tau\cos\tau$	$E = d\sin\gamma + e\cos\gamma$	$e = (\epsilon_2 - \epsilon_3 + \alpha\cos^2\theta)\cos\xi\sin\xi$
$FF = C\sin^2\tau + 2E\cos\tau\sin\tau + F\cos^2\tau$	$F = f$	$f = (\epsilon_2 + \alpha\cos^2\theta)\sin^2\xi + \epsilon_3\cos^2\xi$

ϵ_{11}, ϵ_{22}, and ϵ_{33} represent real parts of the x, y, z dielectric constants of the bilayer. α describes the complex part of the bilayer dielectric tensor with θ accounting for the angle between the main absorption dipole of the chromophore and the plane of the bilayer. γ, ξ, and τ are the rotational degrees of freedom representing the bilayer tilt, the rotational diffusion in the bilayer Brown (1972), and outer segment as a whole.

standard 4×4 matrix technique (Azzam & Bashara, 1987). From the calculations of the transmitted intensity, the spectral absorbance can be deduced for the transverse illumination of the outer segments. Further, by comparing the calculated effective dichroic ratio of the cell, Δ^{cell}, to the dichroic ratios of the bilayers, Δ^{bilayer}, the dichroic factor, Ξ, due to the form birefringence can be found as

$$\Delta^{\text{cell}} = \Xi\Delta^{\text{bilayer}}, \tag{13}$$

3. Calculations of spectral absorbance

The validity of all theoretical predictions depends strongly on the accuracy of the parameters used in the calculations. Liebman (1975) had previously measured the refractive index of the cytoplasm to be 1.365 in outer segments of rods from *Rana pipiens*. At a similar time Liebman, Jagger, Kaplan, and Bargoot (1974) measured the average refractive index and birefringence of the bilayers in the outer segment to be 1.475 and 0.005. However, these values were revised slightly with subsequent measurements (Kaplan, Deffebach, & Liebman, 1978) to values of 1.496 ± 0.018 and 1.488 ± 0.018 for $\text{Re}(\sqrt{\epsilon^1_{11}})$ and $\text{Re}(\sqrt{\epsilon^1_{22}})$, respectively. The higher values reported by Kaplan et al. (1978) fit with the knowledge that protein-containing membranes generally exhibit higher refractive indices (Salamon, Huang, Cramer, & Tollin, 1998) than those that contain lipids alone. For example, Ramsden (1999) showed that two model lipid bilayers had refractive indices of 1.398 and 1.4039 for 1,2-dimyristoleoyl-*sn*-glycero-3-phosphatidylcholine (DMPC) and 1.415 and 1.419 for 1,2-dioleoyl-*sn*-glycero-3-phosphatidylcholine (DOPC). Coupled plasmon waveguide spectroscopy measurements (Salamon et al. (1998)) showed that inclusions such as cytochrome b_6f in similar phosphatidylcholine (PC) model bilayers raised the refractive indices to 1.548 ± 0.001 and 1.480 ± 0.001. Ellipsometry measurements have also shown that inclusions of cholesterol raise PC model bilayer refractive indices to around 1.471 and 1.490 (Jian, Akahane, & Tako, 1981).

In assessing the dichroic factor Ξ as a function of the bilayer refractive indices in the following calculations, a range of values were therefore chosen spanning the results of Kaplan et al. (1978). A refractive index ratio, X, is used to describe this range of values, and is defined as the ratio between the real parts of the bilayer refractive index perpendicular to the plane of that bilayer, $n^1_\perp$, and the cytoplasm, n^2, refractive index. Therefore a refractive index ratio of $X = 1.09$ represents the exact measurements of Kaplan et al. (1978). As regards the dispersion in both the real and imaginary parts of the dielectric tensor of the bilayer, there is very little data in the literature. In the calculations in this work the real parts of the refractive indices were approximated to be independent of wavelength whilst the complex dispersion in the bilayer refractive indices was estimated from the results of Chance, Perry, Akerman, and Thorell (1959) and Harosi (1981).

The principal coordinate systems of the real and complex parts of the dielectric tensor are also not coincident. While the chromophore $C_5 - C_{18}$ axis lies at an angle of $21\pm5°$ (Gröbner, Burnett, Choi, Mason, & Watts, 2000) to the plane of the membrane, the main absorption dipole is believed to make an angle of $\approx16°$ (Jäger et al., 1997). This information was used to calculate the local biaxial complex dielectric tensor of the bilayer environment (see Eq. (11)) (Roberts & Gleeson, 2004). A range of volume fractions occupied by the bilayers were also used in the following calculations and were generally between 0 and 0.5. This assumption was based on a range spanning the results of Kaplan et al. (1978), who measured a variation in the volume fraction along the axis of a *Rana pipiens* rod outer segment to be 0.28 ± 0.11 to 0.22 ± 0.08. A point of note is that the majority of MSP measurements are made with the cells contained in a hyperosmotic medium. This has the effect of changing the physiological volume fraction of the cells during measurements.

Fig. 2 illustrates a comparison of spectral absorbance calculated for both the individual bilayers (solid line) and the outer segment (dashed line) following the theory set out in this paper of a model rod outer segment. The volume fraction and other parameters employed in the calculation were used as described above and are detailed again in the figure caption. Calculating the dichroic ratios from these plots for both cases, shows the increase as expected in the dichroic ratio due to the form birefringence. In this example the dichroic ratio has increased by a factor of $\Xi\approx1.3$. Roberts and Gleeson (2004) also showed that the dichroic ratio was independent of wavelength. Similarly, the data in

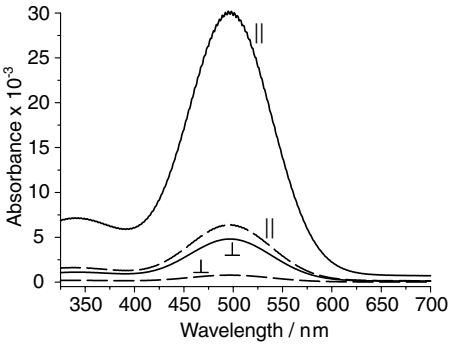

Fig. 2. A comparison between the calculated absorbance spectra for an individual bilayer (solid line) and the outer segment (dashed line) with the incident light polarized both parallel and perpendicular to the plane of the bilayers. Parameters used in the calculation are detailed in Table 1 together with the volume fraction of the bilayers $f = 0.25$ and the ratio between the real parts of the bilayer $n^1_\perp$ and cytoplasm n^2 refractive indices, $X = 1.09$.

Fig. 2 confirms that the dichroic absorbance is independent of wavelength for a general case. Therefore, Ξ is also in general independent of wavelength.

It is immediately apparent from Fig. 2 that the effective optical density of the outer segment is considerably reduced when accounting for the form birefringence, a change not previously considered by other workers. Fig. 3 shows that the effective optical density of the cell is a strong function of the volume fraction occupied by the bilayer. For a volume fraction of 0.25 and a refractive index ratio of $X = 1.09$, the effective optical density of outer segment is only around 25% that of the bilayer. Experimental measures of the optical density (along with measures of the dichroic ratio) are commonly used in the calculation of the visual pigment concentration. Harosi (1982) recognized that in these calculations, the dichroic ratio needed to be corrected for the effects of form birefringence. However, no mention has been made in the literature concerning a similar correction for optical density. Indeed, as form birefringence alters the effective absorbance to change the dichroic ratios, then it seems logical

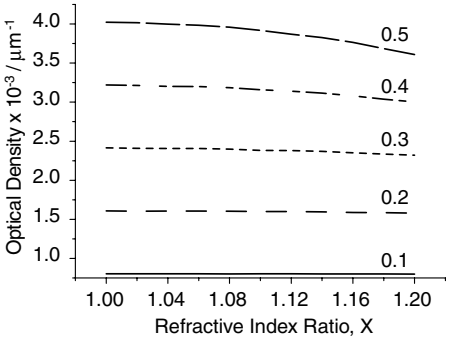

Fig. 3. A graph showing the calculated changes in the perceived optical densities of the outer segments as a function of the ratio, X, between the real parts of the bilayer refractive index $n^1_\perp$ and the cytoplasm n^2 and the volume fractions (labeled) occupied by the bilayers. The optical density of the bilayer is 0.0078 μm^{-1}.

that the absolute values of the measured absorbance and thus the optical density may also change. Clearly from the trend displayed in Fig. 3, uncorrected values of the optical density may lead to a possible underestimation in any calculations of the visual pigment density.

4. Dependency on volume fraction, refractive index ratio, and bilayer birefringence

The above calculations of the absorbance spectra make it straightforward to investigate further the effects of different optical and physical parameters on the dichroic ratios and dichroic factor, Ξ. Fig. 4A illustrates the change in the dichroic factor as a function of both the refractive index ratio and the volume fraction occupied by the bilayers. The profile of the data in Fig. 4A is similar to that published by Israelachvili et al. (1975), and redrawn in Fig. 4B. However, Fig. 4A illustrates that some of the discrepancies from previous theories have now been resolved. The theory derived in this work produces the logically correct result of the dichroism factor Ξ being equal to zero when the volume fraction of the bilayers is zero ($f = 0$) and the outer segment is a uniaxial non-absorbing system.

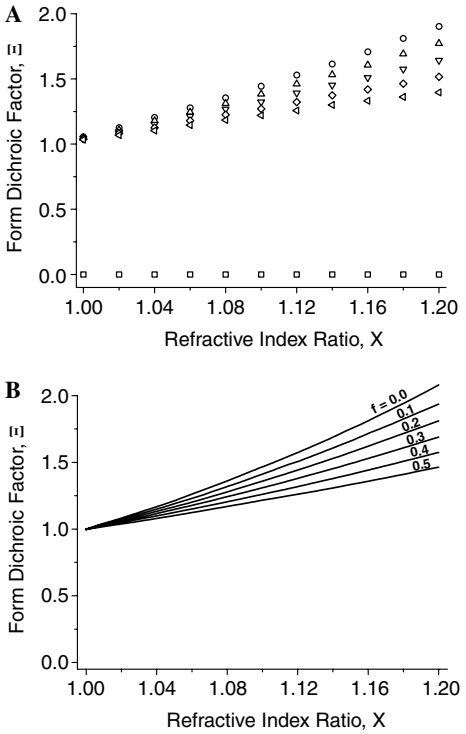

Fig. 4. (A) A graph showing the calculated increase in the dichroic ratio of the outer segment as a function of the ratio, X, between the real parts of the bilayer refractive index $n^1_\perp$ and the cytoplasm n^2. The symbols represent different volume fractions occupied by the bilayers: (□) $f = 0$; (○) $f = 0.1$; (△) $f = 0.2$; (▽) $f = 0.3$; (◇) $f = 0.4$; (◁) $f = 0.5$. (B) A comparison graph showing the change in the dichroic ratio of the outer segment calculated using the theory derived by Israelachvili et al. (1975) (Eq. (16)). Note the increased dichroic factor for no disc membranes present in the outer segment ($f = 0$).

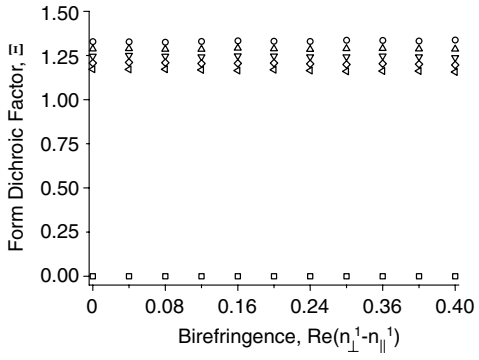

Fig. 5. A graph showing the calculated increase in the dichroic ratio of the outer segment as a function of the intrinsic birefringence $\mathrm{Re}(n_{\perp}^{1} - n_{\parallel}^{1})$. The symbols represent different volume fractions occupied by the bilayers: (□) $f = 0$; (○) $f = 0.1$; (△) $f = 0.2$; (▽) $f = 0.3$; (◇) $f = 0.4$; (◁) $f = 0.5$.

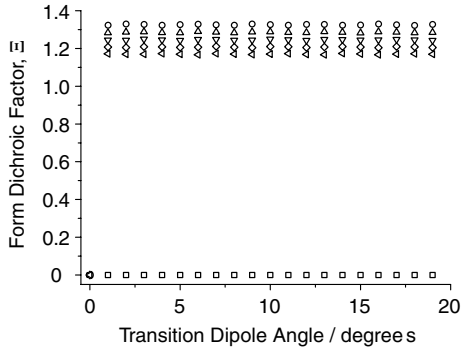

Fig. 6. A graph showing the calculated increase in the dichroic ratio of the outer segment as a function of the angle between the absorption dipole and the plane of the bilayer, defined as γ in Roberts and Gleeson (2004), and representing a function of $\mathrm{Im}(n_{\perp}^{1} - n_{\parallel}^{1})$. Symbols represent different volume fractions occupied by the bilayers: (□) $f = 0$; (○) $f = 0.1$; (△) $f = 0.2$; (▽) $f = 0.3$; (◇) $f = 0.4$; (◁) $f = 0.5$.

Figs. 5 and 6 examine the effects of two further optical parameters on the absorbance spectra. Fig. 5 shows that changes in the intrinsic birefringence of the bilayers, $\mathrm{Re}(n_{\perp}^{1} - n_{\parallel}^{1})$ have little effect on the dichroic factor Ξ. Similarly changes in the angle between the main transition dipole and the plane of the bilayers, i.e., an effective change in $\mathrm{Im}(n_{\perp}^{1} - n_{\parallel}^{1})$ also has little influence on the dichroic factor. Both sets of data indicate, therefore, that the dichroic factor is only a function of the volume fraction occupied by the bilayers and the refractive index difference across the cytoplasm and bilayer interface.

5. Role in polarization sensitivity

To place this work in a wider context, it is worth considering the role that form birefringence may play within the vision process, and in particular the effect it may have on polarized light discrimination and sensitivity. It has been categorically shown that several classes of vertebrate exhibit differing forms of polarization vision (Able & Able, 1995; Freake, 1999; Hawryshyn & McFarland, 1987; Horváth & Varjú, 2004; Phillips, Deutschlander, Freake, & Borland, 2001; Taylor & Adler, 1973), with the majority of the work examining polarization sensitivity in a variety of species of teleosts (Coughlin & Hawryshyn, 1995; Flamarique & Browman, 2001; Flamarique & Hawryshyn, 1997, 1998; Flamarique, Hawryshyn, & Harosi, 1998; Hawryshyn & McFarland, 1987; Parkyn & Hawryshyn, 1993, 2000). However, the underlying mechanisms that cause individual photoreceptors to produce a differential response to different polarizations of light still remain unclear. Several studies (Fineran & Nicol, 1978; Flamarique & Hawryshyn, 1998; Flamarique et al., 1998; Flamarique & Harosi, 2002) have linked transverse dichroic absorbance in certain classes of cone photoreceptors to polarization sensitivity in two families of teleosts.

Fineran and Nicol (1978) provided the first evidence of the unique photoreceptor structure in the anchovy family. *Anchoa mitchilli* and *Anchoa hepsetus* posses a cone photoreceptor type of combined long and bilobed cones where the planes of the bilayer membranes are oriented parallel to the long axis of the outer segments. Flamarique and Harosi (2002) measured the dichroic ratios of the long cone to be about 1.5. A similar photoreceptor structure has also been described in species of *Engraulis mordax* and Flamarique and Hawryshyn (1998) measured the polarization sensitivity from compound action potential recordings in the optic nerve. These measurements showed that the cones did indeed mediate polarization information at the peak wavelength of the spectral response curve. The polarization sensitivity was measured to be 2.57 with the cones having a maximum sensitivity to horizontally polarized light.

The second mechanism that relies on transverse absorbance for polarization sensitivity is a model proposed by Flamarique et al. (1998) in species of salmonid. Several electrophysiological studies have shown significant levels of polarization sensitivity at UV wavelengths in both the optic nerve (Parkyn & Hawryshyn, 1993, 2000) and torus semicircularis (Coughlin & Hawryshyn, 1995) of different species. For the UV cones in the retina to provide such polarization discrimination, Flamarique et al. (1998) suggested that grazing anisotropic reflections from double cone inner segments transversely reflect onto the outer segments of the UV cones.

For a polarization sensitivity mechanism relying on transverse absorbance, any increase in the dichroic ratio would result in a corresponding increase in the differential output from the cell. In fact, it is relatively straightforward to show this mathematically. In terms of the absorbance A, the intensity of light absorbed I_A, can be written as

$$I_A = I_0(1 - 10^{-A}), \tag{14}$$

where I_0 is the incident intensity. The level of polarization sensitivity can be calculated by measuring a threshold level response of the photoreceptor for the different polarizations (Parkyn & Hawryshyn, 1993, 2000). This criterion provides a way of measuring the different incident intensities of polarized light required to produce the same

response or same amount of light absorbed. In these terms, sensitivity, S is defined as (Parkyn & Hawryshyn, 2000)

$$S = -\log(I_0). \tag{15}$$

The polarization sensitivity, PS, can then be written as

$$\mathrm{PS} = 10^{S_\parallel - S_\perp} = \frac{I_{0\perp}}{I_{0\parallel}} \tag{16}$$

for sensitivity to light polarized parallel, $S_\parallel$ and perpendicular, $S_\perp$ to the plane of the bilayer. The polarization sensitivity can therefore be equated with the absorbance as

$$\mathrm{PS} = \frac{(I_A/I_{0\parallel})}{(I_A/I_{0\perp})} = \frac{1-10^{-A_\parallel}}{1-10^{-A_\perp}}, \tag{17}$$

which for values of absorbance $\ll 1$ can be approximated by the simple relationship

$$\mathrm{PS} \approx \frac{A_\parallel}{A_\perp} = \text{Dichroic ratio}. \tag{18}$$

It is within this relationship that form birefringence plays its role in the vision process. Fig. 4 illustrated that form birefringence increases the transverse dichroic ratio of the outer segments. Therefore, by Eq. (18), increasing the level of form birefringence will increase the polarization sensitivity of an individual photoreceptor for a transversely absorbing mechanism. However, decreasing the volume fraction of the bilayers within the outer segment to increase the dichroic ratio would have the adverse effect of decreasing the optical density. Consequently, in a system that is designed for polarization discrimination using this mechanism, a balance must exist between efficiency of photon detection and the level of polarization contrast.

As an interesting extra point, it is worth noting that the dichroic ratios of individual cones have also been compared to levels of polarization sensitivity at later stages of neural processing with compound action potential recordings made in the optic nerve in the same species. For example, dichroic ratio measurements in goldfish (*Carassius auratus*) cone photoreceptors have been made by Harosi and MacNichol (1974). Across the long, mid, and short wavelength cone types, the dichroic ratios were found to be in the range of 2–3. In comparison, Hawryshyn and McFarland (1987) measured polarization sensitivity of the UV, mid, and long wavelength cone mechanisms to be 4.68 from compound action potential recordings in the optic nerve. These values are approximately double the dichroic ratio values. This gain in the sensitivity to polarized light has been highlighted as evidence for the role of synaptic inhibition to improve the efficiency of discrimination. Undoubtedly, in mechanisms of transverse polarized light detection, form birefringence and these neural levels polarization sensitivity are related through several stages of complex processing. However, important studies are still needed to understand this relationship.

Furthermore, to the author's knowledge there have been no conclusive experimental measurements of form birefringence. Although, in a comment made by Snyder (1978), he indicated that Liebman and Bargoot had found the dichroic factor to be at least 1.2. Even with new experimental techniques and technology, definitive information on the how the structure of the outer segments influences the absorbance of polarized light remains an exciting challenge.

6. Conclusions

In summary, a new theoretical model has been derived enabling a precise calculation of the absorbance spectra of transversely illuminated photoreceptor outer segments. The occurrence of form birefringence in the periodic bilayer/cytoplasm lamellar structure significantly affects the way polarized light is absorbed transversely, particularly in changing the values of the cellular dichroic ratios. The increase with respect to the dichroic ratio value when the form birefringence is not considered is seen to be ≈ 1.3 for physiologically realistic parameters. Importantly, the results derived from this work have exhibited none of the inconsistencies evident in previously published theories. Furthermore, these calculations suggest that experimental measurements of optical density may need to take into account form birefringence in order to provide accurate results.

Acknowledgments

The financial support of the Leverhulme Foundation is gratefully acknowledged. The author also wishes to thank H.F. Gleeson, M.R. Dickinson and two anonymous reviewers for comments on the manuscript.

References

Able, K. P., & Able, M. A. (1995). Manipulations of polarized skylight calibrate magnetic orientation in a migratory bird. *Journal of Comparative Physiology A, 177*, 351–356.

Azzam, R. M., & Bashara, N. M. (1987). *Ellipsometry and polarised light*. Amsterdam: Elsevier, p. 340.

Bêche, B., & Gaviot, E. (2003). Matrix formalism to enhance the concept of effective dielectric constant. *Optics Communications, 219*, 15–19.

Born, M., & Wolf, E. (1999). *Principles of optics* (7th ed.). Cambridge: Cambridge University Press, p. 837.

Brown, P. (1972). Rhodopsin rotates in the visual receptor membrane. *Nature New Biology, 236*, 35.

Chance, B., Perry, R., Akerman, L., & Thorell, B. (1959). Highly sensitive recording microspectrophotometer. *The Review of Scientific Instruments, 30*, 735–741.

Coughlin, D. J., & Hawryshyn, C. W. (1995). A cellular basis for polarized-light vision in rainbow trout. *Journal of Comparative Physiology A, 176*, 261–272.

Fineran, B. A., & Nicol, J. A. C. (1978). Studies of the photoreceptors of *Anchoa mitchilli* and *A. hepsetus* (Engraulidae) with particular reference to the cones. *Philosophical Transactions of the Royal Society of London. Series B, 283*, 26–60.

Flamarique, I. N., & Browman, H. I. (2001). Foraging and prey-search behaviour of small juvenile rainbow trout (*Onchorhynchus mykiss*) under polarized light. *The Journal of Experimental Biology, 204*, 2415–2422.

Flamarique, I. N., & Harosi, F. I. (2002). Visual pigments and dichroism of anchovy cones: A model system for polarization detection. *Visual Neuroscience, 19*, 467–473.

Flamarique, I. N., & Hawryshyn, C. W. (1997). Is the use of underwater polarized light by fish restricted to crepuscular time periods? *Vision Research, 37*, 975–989.

Flamarique, I. N., & Hawryshyn, C. W. (1998). Photoreceptor types and their relation to the spectral and polarization sensitivities of clupeid fishes. *Journal of Comparative Physiology A, 182*, 793–803.

Flamarique, I. N., Hawryshyn, C. W., & Harosi, F. I. (1998). Double-cone internal reflection as a basis for polarization detection in fish. *Journal of the Optical Society of America A, 15*, 349–358.

Freake, M. J. (1999). Evidence for orientation using the e-vector direction of polarized light in the sleepy lizard *Tiliqua rugosa*. *The Journal of Experimental Biology, 202*, 1159–1166.

Gröbner, G., Burnett, C. G., Choi, A., Mason, J., & Watts, A. (2000). Observations of light-induced structural changes of retinal within rhodopsin. *Nature, 405*, 801–813.

Haggins, W. A., & Jennings, W. A. (1959). Radiationless migration of electronic excitation in retinal rods. *Discussions of the Faraday Society, 27*, 180–190.

Harosi, F. I. (1975). Linear dichroism of rods and cones. *NATO Advanced Science Institutes Series A*, 55–65.

Harosi, F. I. (1978). Comments on form dichroism in vertebrate photoreceptors. *Vision Research, 18*, 353–354.

Harosi, F. I. (1981). Microspectrophotometry and optical phenomena: Birefringence, dichroism and anomalous dispersion. In J. M. Enoch & F. L. Tobey, Jr. (Eds.), *Vertebrate photoreceptor optics* (pp. 337). Berlin: Springer.

Harosi, F. I. (1982). Polarized microspectrophotometry for pigment orientation and concentration. In L. Paker (Ed.), *Methods in enzymology* (pp. 642–647). New York: Academic Press.

Harosi, F. I., & MacNichol, E. F. Jr., (1974). Visual Pigments of goldfish cones: Spectral properties and dichroism. *The Journal of General Physiology, 63*, 279–304.

Harosi, F. I., & Malerba, F. E. (1975). Plane polarized light in microspectrophotometry. *Vision Research, 15*, 379–388.

Hawryshyn, C. W., & McFarland, W. N. (1987). Cone photoreceptor mechanisms and the detection of polarized light in fish. *Journal of Comparative Physiology A, 160*, 459–465.

Horváth, G., & Varjú, D. (2004). *Polarized light in animal vision*. Berlin: Springer, pp. 293–354.

Israelachvili, J. N., Sammut, R. A., & Snyder, A. W. (1975). Birefringence and dichroism of photoreceptors. *Vision Research, 16*, 47–52.

Jäger, S., Lewis, J. W., Zvyaga, T. A., Szundi, I., Sakmar, T. P., & Kliger, D. S. (1997). Chromophore structural changes in rhodopsin from nanoseconds to microseconds following pigment photolysis. *Proceedings of the National Academy of Sciences of the United States of America, 94*, 8557–8562.

Jian, W.-L., Akahane, T., & Tako, T. (1981). Optical properties of oxidized cholesterol bilayer lipid membranes. *Molecular Crystals and Liquid Crystals, 69*, 3–18.

Kaplan, M. W., Deffebach, M. E., & Liebman, P. A. (1978). Birefringence measurements of structural inhomogeneities in *Rana pipiens* rod outer segments. *Biophysical Journal, 23*, 59–70.

Laughlin, S. B., Menzel, R., & Snyder, A. W. (1975). Membranes, dichroism and receptor sensitivity. In A. W. Snyder & R. Menzel (Eds.), *Photoreceptor optics* (pp. 237). Berlin: Springer.

Liebman, P. A. (1962). In situ microspectrophotometric studies on the pigments of single retinal rods. *Biophysical Journal, 2*, 161–178.

Liebman, P. A. (1975). Birefringence, dichroism and rod outer segment structure. In A. W. Snyder & R. Menzel (Eds.), *Photoreceptor optics* (pp. 119). Berlin: Springer.

Liebman, P. A., Jagger, W. S., Kaplan, M. W., & Bargoot, F. G. (1974). Membrane structure changes in rod outer segments with rhodopsin bleaching. *Nature, 251*, 31–36.

Moody, M. F. (1964). Photoreceptor organelles in animals. *Biological Reviews, 39*, 43–86.

Parkyn, D. C., & Hawryshyn, C. W. (1993). Polarized-light sensitivity in rainbow trout (*Oncorhyncbus mykiss*): Characterization from multi-unit responses in the optic nerve. *Journal of Comparative Physiology A, 172*, 493–500.

Parkyn, D. C., & Hawryshyn, C. W. (2000). Spectral and ultraviolet-polarization sensitivity in juvenile salmonids: A comparative analysis using electrophysiology. *The Journal of Experimental Biology, 203*, 1173–1191.

Phillips, J. B., Deutschlander, M. E., Freake, M. J., & Borland, C. (2001). The role of extraocular photoreceptors in newt magnetoreception and polarized light detection in vertebrates. *The Journal of Experimental Biology, 204*, 2543–2552.

Ramsden, J. J. (1999). Molecular orientation in lipid bilayers. *Philosophical Magazine B, 79*, 381–386.

Roberts, N. W., & Gleeson, H. F. (2004). The absorption of polarized light by vertebrate photoreceptors. *Vision Research, 44*, 2643–2652.

Roberts, N. W., Temple, S. E., Haimberger, T. J., Gleeson, H. F., & Hawryshyn, C. W. (2004). Differences in the optical properties of vertebrate photoreceptor classes leading to axial polarization sensitivity. *Journal of the Optical Society of America A, 21*, 335–345.

Salamon, Z., Huang, D., Cramer, W. A., & Tollin, G. (1998). Coupled plasmon-waveguide resonance spectroscopy studies of the cytochrome b_6f/plastocyanin system in supported lipid bilayer membranes. *Biophysical Journal, 75*, 1874–1885.

Snyder, A. W. (1978). Comments on form dichroism in vertebrate photoreceptors—reply. *Vision Research, 18*, 355–356.

Snyder, A. W., & Laughlin, S. B. (1975). Dichroism and absorption by photoreceptors. *Journal of Comparative Physiology, 100*, 101–116.

Taylor, D. H., & Adler, K. (1973). The pineal body: Site of extraocular perception of celestial cues for orientation in the tiger salamander (*Ambystoma tigrinum*). *Journal of Comparative Physiology A, 124*, 357–361.

Weale, R. A. (1971). On the linear dichroism of frog rods. *Vision Research, 11*, 1373–1385.

Wiener, O. (1912). Die theorie des mischkörpers für das feld der stationären stromüng. *Abh. Math. Phys. Kl. Königl. Sächs. Ges. Wiss., 32*, 507–604.